nature immunology

HIV-1 blocks the signaling adaptor MAVS to evade antiviral host defense after sensing of abortive HIV-1 RNA by the host helicase DDX3

Sonja I Gringhuis, Nina Hertoghs, Tanja M Kaptein, Esther M Zijlstra-Willems, Ramin Sarrami-Fooroshani, Joris K Sprokholt, Nienke H van Teijlingen, Neeltje A Kootstra, Thijs Booiman, Karel A van Dort, Carla M S Ribeiro, Agata Drewniak & Teunis B H Geijtenbeek

The mechanisms by which human immunodeficiency virus 1 (HIV-1) avoids immune surveillance by dendritic cells (DCs), and thereby prevents protective adaptive immune responses, remain poorly understood. Here we showed that HIV-1 actively arrested antiviral immune responses by DCs, which contributed to efficient HIV-1 replication in infected individuals. We identified the RNA helicase DDX3 as an HIV-1 sensor that bound abortive HIV-1 RNA after HIV-1 infection and induced DC maturation and type I interferon responses via the signaling adaptor MAVS. Notably, HIV-1 recognition by the C-type lectin receptor DC-SIGN activated the mitotic kinase PLK1, which suppressed signaling downstream of MAVS, thereby interfering with intrinsic host defense during HIV-1 infection. Finally, we showed that PLK1-mediated suppression of DDX3–MAVS signaling was a viral strategy that accelerated HIV-1 replication in infected individuals.

Dendritic cells (DCs) are crucial in the induction of adaptive immune responses to infection with HIV-1 (ref. 1); however, DCs do not mount protective immunity against HIV-1 (ref. 2), which is attributed to the ability of HIV-1 to escape immune surveillance.

DCs sense invading viruses through pattern-recognition receptors (PRRs) that trigger type I interferon (IFN) and cytokine responses that lead to intrinsic antiviral defenses and adaptive immunity[1]. Type I interferon responses are induced when IFN-α and IFN-β, via autocrine signaling, activate an antiviral program of interferon-stimulated genes (ISGs) that counteract virus replication[3–5]. However, type I interferons also induce antiviral adaptive immunity via DC maturation[6] and T helper cell polarization[7]. Although HIV-1 infects DCs efficiently, neither DC activation nor type I interferon responses are induced[2]. Type I interferon responses early during infection lower susceptibility to simian immunodeficiency virus (SIV) infection in rhesus macaques and slow disease progression[8]. These observations strongly suggest that the absence of type I interferon responses underlie the lack of protective immunity during HIV-1 infection.

During the life cycle of HIV-1, various classes of host PRRs encounter different HIV-1 ligands that could potentially trigger type I interferon responses. The C-type lectin receptor DC-SIGN recognizes the HIV-1 envelope protein gp120, which triggers signaling mediated by the serine–threonine kinase Raf-1 (refs. 9,10). The cytosolic receptor RIG-I recognizes purified HIV-1 single-stranded RNA (ssRNA), but it remains unclear whether this interaction also occurs during infection[11]. Toll-like receptor 8 (TLR8) recognizes HIV-1 ssRNA after endosomal degradation of virions, thereby inducing activation of the transcription factor NF-κB[12]. HIV-1 exploits cooperative DC-SIGN and TLR8 signaling in DCs for transcription initiation and elongation[12]. NF-κB initiates transcription from the integrated provirus; however, RNA polymerase is unable to proceed beyond the first 58 nucleotides, generating 'abortive' HIV-1 RNAs[12,13]. DC-SIGN-induced Raf-1 activation leads to recruitment of transcription elongation factor pTEF-b, which modulates RNA polymerase, and transcription proceeds to generate full-length functional HIV-1 transcripts that contain poly(A) tails[12]. These full-length transcripts remain unspliced or are processed into multiply or singly spliced transcripts; all are exported from the nucleus into the cytoplasm. Several DEAD box RNA helicases related to RIG-I, such as DDX1, DDX3 and DDX5, assist in nuclear export of HIV-1 transcripts[14,15]. DDX3 is also involved in translation of HIV-1 transcripts via direct binding to the 5′ m^7GTP cap structure of HIV-1 transcripts[16]. A highly ordered process results in the assembly of translation initiation complexes consisting of trimeric complexes of DDX3 with translation initiation factor eIF4G and poly(A)-binding protein (PABP), as well as translation initiation factor eIF4A[16,17]. These complexes allow 43S ribosomal units to attach to the transcripts to ultimately mediate *de novo* synthesis of viral proteins[16,17]. HIV-1 cDNA, generated during reverse transcription, is recognized by the DNA sensor cyclic GMP–AMP synthase (cGAS), which, via the membrane-associated adaptor protein STING, leads to activation of the transcription factor IRF3 that drives IFN-β

Department of Experimental Immunology, Academic Medical Center, University of Amsterdam, Amsterdam, the Netherlands. Correspondence should be addressed to S.I.G. (s.i.gringhuis@amc.uva.nl) or T.B.H.G. (t.b.geijtenbeek@amc.uva.nl).

Received 21 July; accepted 30 November; published online 26 December 2016; doi:10.1038/ni.3647

expression[18,19]. HIV-1 escapes detection by cGAS because host proteins, such as the cytosolic exonuclease TREX1, which digests HIV-1 DNA[20], and the phosphohydrolase SAMHD1, which limits the generation of HIV-1 DNA[21], limits the amount of viral DNA in the cell. However, SAMHD1-mediated restriction of DC infection does not account for the lack of DC activation[22]. Thus, although viral RNA, DNA and proteins are recognized by various host proteins, it remains unclear how HIV-1 avoids immune surveillance in DCs.

Here we identified the RNA helicase DDX3 as a sensor for abortive HIV-1 RNA in DCs, which induced type I interferon responses and DC maturation via the signaling adaptor protein MAVS. However, simultaneous recognition of HIV-1 by DC-SIGN suppressed these responses via Raf-1-mediated activation of host factor PLK1, which impeded signaling downstream of MAVS. The identification of a rare dual MAVS(Q198K,S409F) mutant that is resistant to PLK1 inactivation, which thereby contributed to limiting the viral RNA load, demonstrated the significance of DDX3-mediated sensing for HIV-1 replication in infected individuals.

RESULTS

HIV-1 innate signaling via Raf-1 blocks type I interferon responses

Because HIV-1 activates Raf-1 (ref. 12), we investigated whether Raf-1 is involved in the suppression of type I interferon responses after HIV-1 infection of human DCs. Monocyte-derived DCs (moDCs) did not express *IFNB* mRNA (which encodes IFN-β) after infection with the laboratory R5-tropic strain HIV-1_{BaL}; however inhibition of Raf-1 activity with the small-molecule inhibitor GW5074 or silencing of Raf-1 expression by RNA interference (RNAi) induced transient expression of *IFNB* transcripts, which peaked at 4 h after infection, (**Fig. 1a**,**b**). Treatment with GW5074 also induced transient expression of various ISGs, such as *ISG15*, *MX2*, *TRIM5*, *TRIM22* and *APOBEC3G* (**Fig. 1c**); however, it did not affect TLR4-induced *IFNB* expression in moDCs (**Supplementary Fig. 1**). Infection with HIV-1_{BaL} induced *IFNB* expression in only GW5074-treated but not untreated human primary myeloid, dermal, intestinal and vaginal DCs isolated from blood, skin, intestinal and vaginal tissues, respectively (**Fig. 1d**). We also observed *IFNB* expression after infection of GW5074-treated moDCs both with different laboratory strains (R5-tropic HIV-1_{SF162} or X4-tropic HIV-1_{R9} and HIV-1_{LAI}) and with primary R5-tropic HIV-1 strains isolated from infected patients (**Fig. 1e**,**f**). These data indicated that, following HIV-1 infection, Raf-1 activation in DCs blocks antiviral type I interferon responses.

HIV-1 infection triggers type I interferon responses via DDX3

Induction of *IFNB* expression in GW5074-treated HIV-1_{BaL}-infected moDCs was abrogated by treatment with the reverse-transcriptase inhibitor azidothymidine (AZT; a nucleoside analog) or the integrase inhibitor raltegravir (RAL), or by silencing of TLR8 expression using RNAi (**Fig. 2a**). Because the sensing of HIV-1 ssRNA by TLR8 is crucial to the initiation of HIV-1 transcription[12], these data suggested that type I interferon responses are triggered by HIV-1 RNA transcripts. Silencing of the expression of the cDNA sensor cGAS (encoded by *MB21D1*) and its downstream effector STING (encoded by *TMEM173*)[18,19] by RNAi did not affect *IFNB* expression in GW5074-treated HIV-1_{BaL}-infected moDCs (**Fig. 2b** and **Supplementary Fig. 2**). HIV-1_{BaL} infection induced *IFNB* expression in both untreated and GW5074-treated moDCs after *TREX1* silencing by RNAi, and this was abrogated after silencing the expression of either cGAS or STING, as well as by treatment with the reverse transcriptase inhibitor AZT but not the integrase inhibitor RAL (**Fig. 2b** and **Supplementary Fig. 2**). GW5074 treatment further enhanced *IFNB* expression in *TREX1*-silenced HIV-1_{BaL}-infected moDCs (**Fig. 2b** and **Supplementary Fig. 2**). Thus, there are at least two independent HIV-1-sensing pathways in DCs, a Raf-1-sensitive pathway triggered by an RNA sensor after HIV-1 transcription and the TREX1-sensitive pathway induced by the DNA sensor cGAS after reverse transcription.

To identify the RNA sensor, we silenced the expression of the RNA helicases RIG-I (encoded by *DDX58*) and MDA5 (encoded by *IFIH1*), which did not interfere with *IFNB* expression in GW5074-treated HIV-1_{BaL}-infected moDCs (**Supplementary Fig. 2**). Silencing the expression of DDX3 (encoded by *DDX3X*), but not DDX1 or DDX5, by RNAi abrogated *IFNB* expression in GW5074-treated HIV-1_{BaL}-infected moDCs (**Fig. 2c**). *IFNB* expression was not affected by silencing of DDX3 expression in *TREX1*-silenced HIV-1_{BaL}-infected moDCs or by stimulation of moDCs with ligands specific for RIG-I–MDA5, cGAS–STING or TLR4 (**Supplementary Fig. 2**). Rescue of DDX3 expression by transfection of a DDX3-encoding plasmid restored *IFNB* expression in *DDX3X*-silenced GW5074-treated HIV-1_{BaL}-infected moDCs (**Fig. 2d**), excluding off-target silencing effects. These data strongly suggested

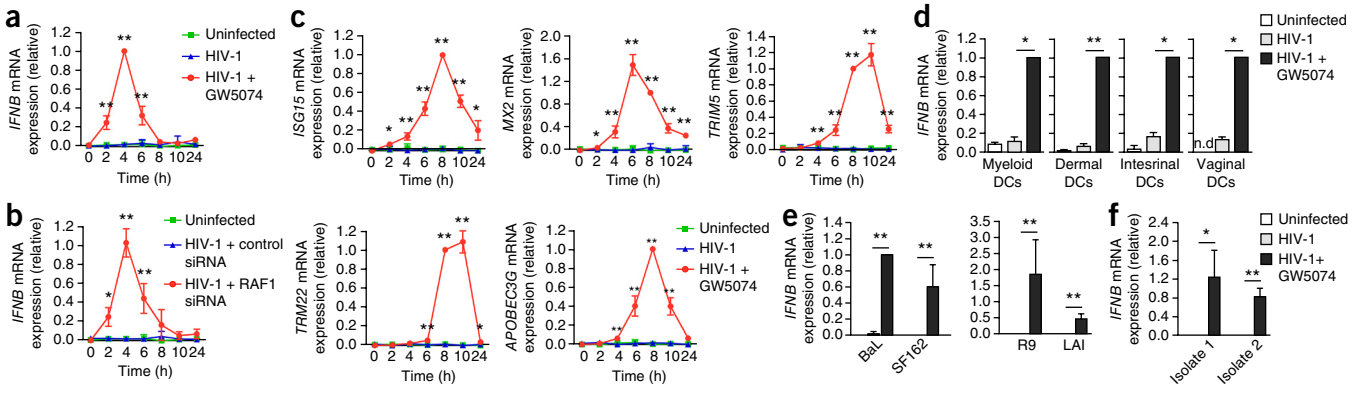

Figure 1 Raf-1 activation suppresses type I IFN responses after HIV-1 infection of DCs. (**a**–**f**) Real-time PCR (RT–PCR) analyses of *IFNB* (**a**,**c**–**f**), and of *ISG15*, *MX2*, *TRIM5*, *TRIM22* and *APOBEC3G* (**b**) mRNA in monocyte-derived (**a**–**c**,**e**,**f**) or primary (**d**) DCs after infection (as indicated (**a**–**c**) or 4 h (**d**–**f**)) with the R5-tropic laboratory strain HIV-1_{BaL} (**a**–**e**), the R5-tropic laboratory strain HIV-1_{SF162} and the X4-tropic laboratory strains HIV-1_{R9} and HIV-1_{LAI} (**e**) or with primary HIV-1 isolates from infected patients (**f**), in the absence or presence of Raf-1 inhibition (using GW5074 (**a**,**c**–**f**) or by *RAF1* silencing (**b**)). n.d., not determined. Data are mean ± s.d. of six (**a**,**c**,**e**), four (**b**,**f**), two (**d**, myeloid, vaginal, intestinal DCs) or three (**d**, dermal DCs) different donors. $^{**}P < 0.01$ and $^{*}P < 0.05$ (Student's *t*-test).

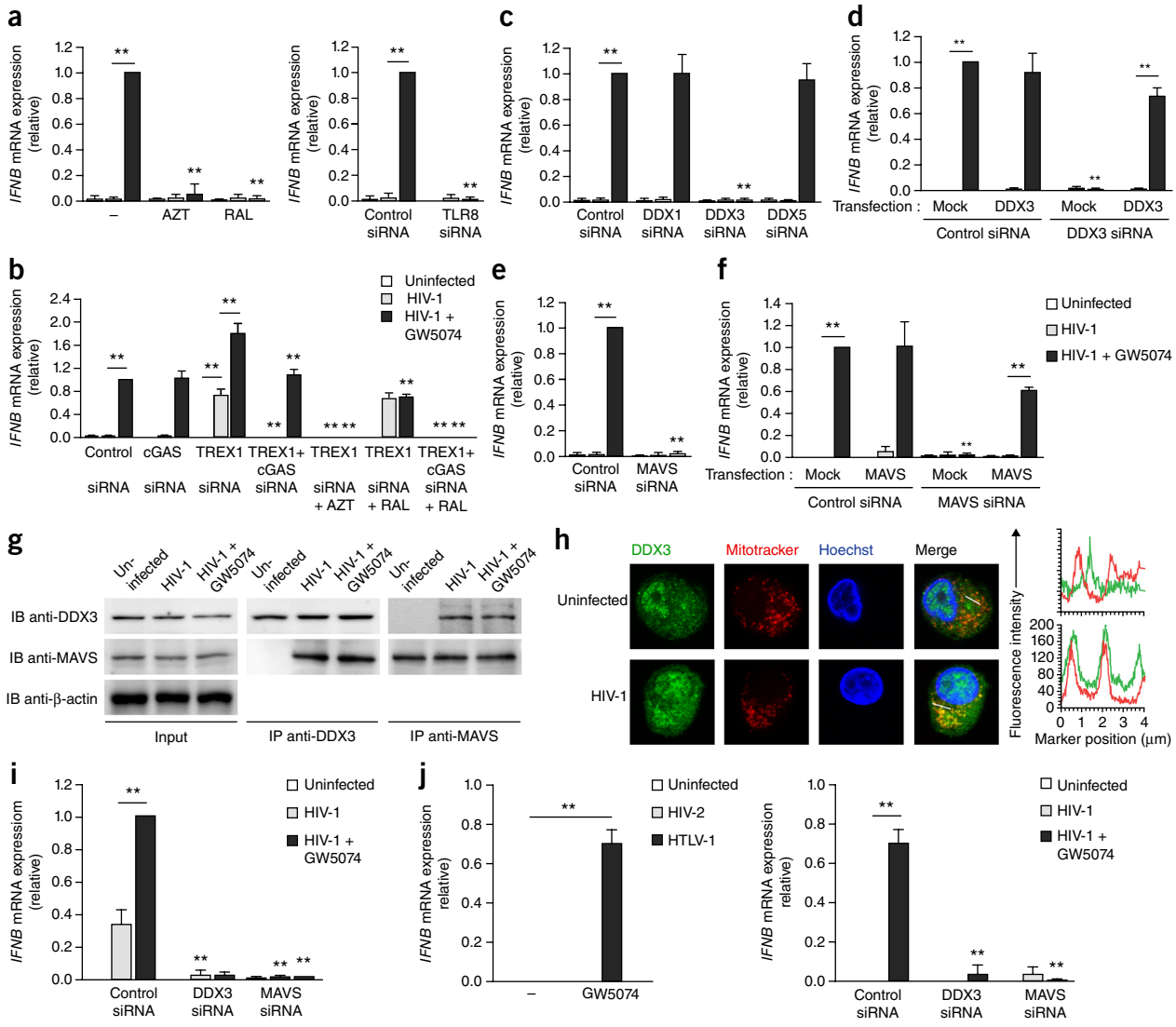

Figure 2 Type I interferon responses after HIV-1 infection are mediated by DDX3–MAVS. (**a**–**f**) RT–PCR analyses of *IFNB* mRNA in moDCs (**a**–**f**) after infection with HIV-1_{BaL} (4 h; **a**–**f**), in the absence or presence of the Raf-1 inhibitor GW5074, the reverse-transcription inhibitor azidothymidine (AZT) or the integrase inhibitor raltegravir (RAL) (**a**,**b**), and/or after silencing (siRNA) of TLR8 (**a**), TREX1 (**b**), cGAS (**b**), DDX1 (**c**), DDX5 (**c**), DDX3 (**c**,**d**) or MAVS (**e**,**f**). In **d**,**f**, expression of DDX3 (**d**) or MAVS (**f**) was rescued by transfection with plasmids expressing RNAi-resistant cDNAs. (**g**) Immunoblot (IB) analyses after immunoprecipitation (IP) of DDX3 or MAVS from untreated and GW5074-treated moDCs that were infected with HIV-1_{BaL} for 3 h. β-actin served as loading control for the IB analyses. (**h**) Left, confocal immunofluorescence analyses of DDX3 and mitochondria (MitoTracker) in moDCs after HIV-1 infection for 3 h. Right, graphs showing fluorescence intensity along the marker (white bars, 4 μm). (**i**,**j**) RT–PCR analyses of *IFNB* mRNA in monocyte-derived macrophages (**i**) or moDCs (**j**) after infection with HIV-1_{BaL} (6 h; **i**), HIV-2_{7312A} or HTLV-1_{MT-2} (4 h; **j**), in the absence or presence of the Raf-1 inhibitor GW5074 and after silencing (siRNA) of DDX3 or MAVS. In **j**, N_t was set at 1 for GW5074-treated HIV-1-infected moDCs (not shown). Data are representative of three independent experiments (**g**,**h**) or are the mean ± s.d. of six (**a**,**c**), three (**b**,**j**), four (**d**,**f**,**i**) and ten (**e**) different donors. $^{**}P < 0.01$ (Student's *t*-test).

that DDX3 is the Raf-1-sensitive HIV-1 sensor in moDCs. We next examined whether DDX3, like other RNA sensors[18], signals via MAVS. Silencing of MAVS expression inhibited *IFNB* expression in GW5074-treated HIV-1_{BaL}-infected moDCs (**Fig. 2e**), which was restored by transfection of a MAVS-encoding plasmid (**Fig. 2f**). Furthermore, MAVS co-immunoprecipitated with DDX3, and vice versa, from whole-cell extracts of both untreated and GW5074-treated HIV-1_{BaL}-infected moDCs, but not from extracts of uninfected moDCs (**Fig. 2g**). Confocal microscopy showed that HIV-1 infection invoked partial colocalization of DDX3 around mitochondria (**Fig. 2h**). Thus, DDX3 triggers type I interferon responses in moDCs via MAVS after HIV-1 infection, and these responses are blocked by a Raf-1-mediated pathway.

In contrast to infection of moDCs, HIV-1_{BaL} infection induced *IFNB* expression in monocyte-derived macrophages, which was further enhanced by GW5074 treatment and completely abrogated after silencing of DDX3 or MAVS expression (**Fig. 2i**), Thus, the DDX3–MAVS sensing mechanism also exists in macrophages. We next examined whether other retroviruses also trigger DDX3. HTLV-1, despite its ability to infect moDCs (**Supplementary Fig. 1**), did not induce *IFNB* responses in either untreated or GW5074-treated moDCs (**Fig. 2j**). In contrast, efficient HIV-2 infection (**Supplementary Fig. 1**) induced *IFNB* expression in GW5074-treated moDCs, which was abrogated after silencing of DDX3 or MAVS expression (**Fig. 2j**). These results imply that triggering of

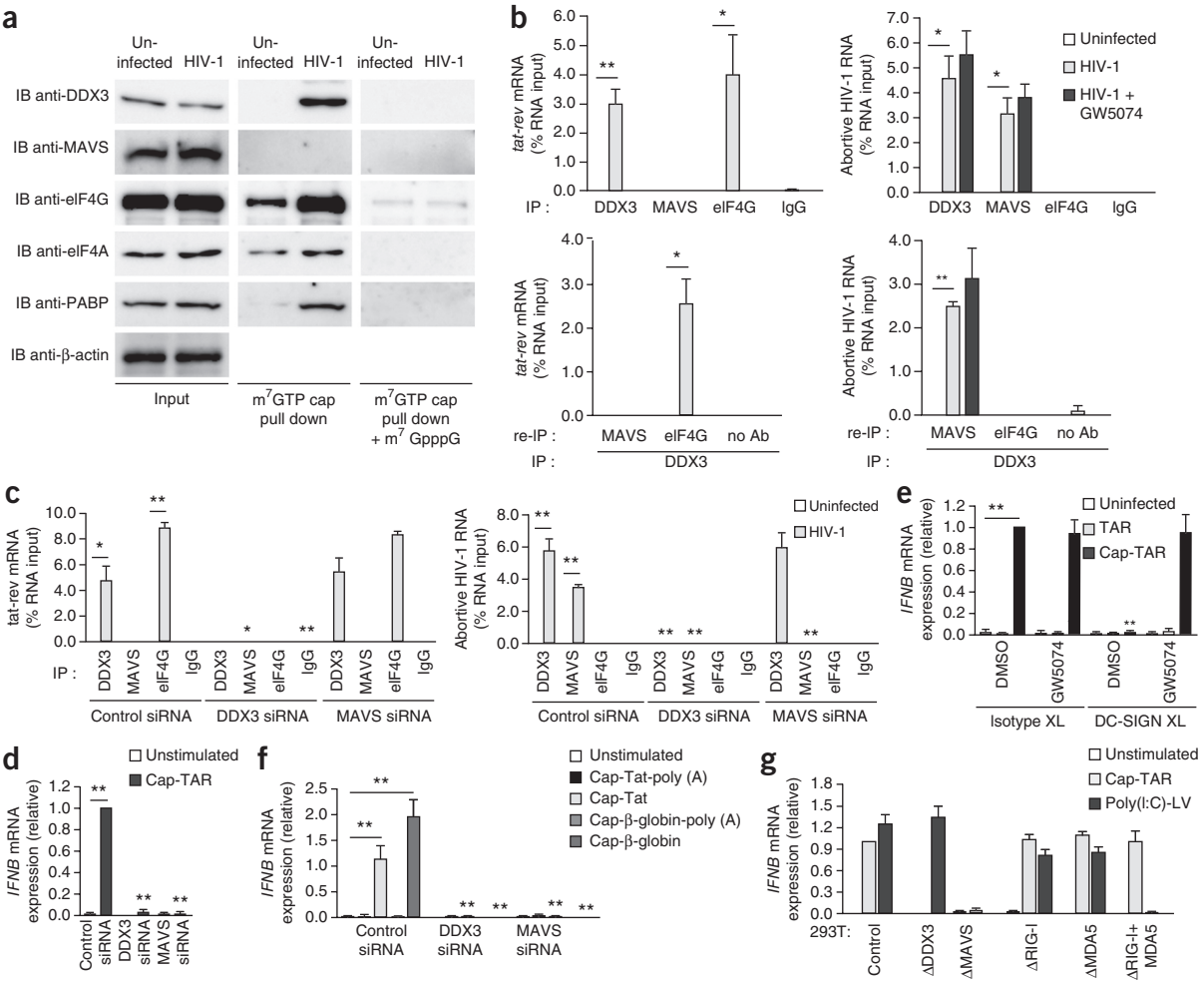

Figure 3 DDX3 bound to capped abortive HIV-1 RNA products induces type I interferon responses via MAVS. (**a**) Immunoblot (IB) analyses of DDX3, MAVS, eIF4G, eIF4A and PABP after pulldown of m^{7}GTP-cap-bound translation initiation complexes from moDCs 3 h after HIV-1_{BaL} infection. The cap analog m^{7}GpppG was used as a competitor. β-actin served as a loading control. (**b**,**c**) RT–PCR analyses of abortive HIV-1 RNA and *tat-rev* HIV-1 mRNA after RNA immunoprecipitation (IP) of DDX3, MAVS or eIF4G from moDCs 3 h after HIV-1_{BaL} infection, in the absence or presence of the Raf-1 inhibitor GW5074 (**b**), or after silencing (siRNA) of DDX3 or MAVS expression in moDCs (**c**). IgG and no antibody (Ab) indicate negative controls. (**d**–**f**) RT–PCR analyses of *IFNB* mRNA in moDCs 4 h after transfection with HIV-1-derived sequences or endogenous human *HBB* RNA sequences, containing or not the 5′m^{7}GTP cap (cap) and/or 3′poly(A) (poly(A)) structures as indicated, after silencing of DDX3 or MAVS expression (**d**,**f**) or after cross-linking (XL) of DC-SIGN, in the absence or presence of GW5074 (**e**). TAR, sequence corresponding to abortive HIV-1 RNA; Tat, sequence corresponding to full-length HIV-1 *tat* transcript; β-globin, sequence corresponding to full-length human *HBB* transcript. (**g**) RT–PCR analyses of *IFNB* mRNA in 293T cells depleted of DDX3, MAVS, RIG-I and/or MDA5 by CRISPR–Cas9 genome editing 4 h after transfection with cap-TAR RNA coupled to LyoVec or with poly(I:C)-LyoVec as a control. Data are representative of three independent experiments (**a**) or are the mean ± s.d. of three (**b**,**c**), eight (**d**) or four (**e**,**f**) different donors or of four independent measurements (**g**). $*P < 0.05$ and $**P < 0.01$ (Student's *t*-test).

the DDX3–MAVS pathway for the induction of type I interferon responses is not a shared feature of all retroviruses, but neither is it restricted to HIV-1.

DDX3 binding to abortive HIV-1 RNA leads to MAVS activation

Considering its role in the translation of HIV-1 transcripts[16,17], we next investigated whether DDX3 associates with MAVS within translation initiation complexes. Translation initiation complexes from nuclease-treated whole-cell extracts were retained on m^{7}GTP-coupled agarose beads and analyzed by immunoblotting; DDX3 but not MAVS associated with eIF4G, eIF4A and PABP within translation initiation complexes in HIV-1_{BaL}-infected, but not uninfected, moDCs (**Fig. 3a**). This result implied that the DDX3 fraction in translation initiation complexes is distinct from the fraction involved in MAVS-dependent signaling. We found that, after either a single RNA immunoprecipitation (RIP) step or following a second RNA immunoprecipitation (re-RIP) step, DDX3 together with eIF4G, but not MAVS, interacted with the viral *tat–rev* mRNA in HIV-1_{BaL}-infected moDCs (**Fig. 3b**). Silencing of DDX3 expression but not MAVS expression by RNAi in moDCs blocked recruitment of eIF4G to *tat–rev* transcripts (**Fig. 3c**). In contrast, DDX3–MAVS but not DDX3–eIF4G complexes bound abortive HIV-1 RNAs in HIV-1_{BaL}-infected moDCs (**Fig. 3b**). *DDX3X* silencing abrogated MAVS recruitment to abortive HIV-1 RNAs, whereas *MAVS* silencing did not interfere with the association between DDX3 and the abortive HIV-1 RNAs (**Fig. 3c**), suggesting that DDX3-dependent sensing of abortive HIV-1 RNAs preceded association of DDX3 with MAVS.

We next transfected moDCs with different HIV-1-derived RNAs, thereby bypassing *IFNB* suppression by DC-SIGN and Raf-1. Transfection of moDCs with abortive HIV-1 RNAs (cap-TAR) induced *IFNB* expression, which was abrogated by the silencing of DDX3 or

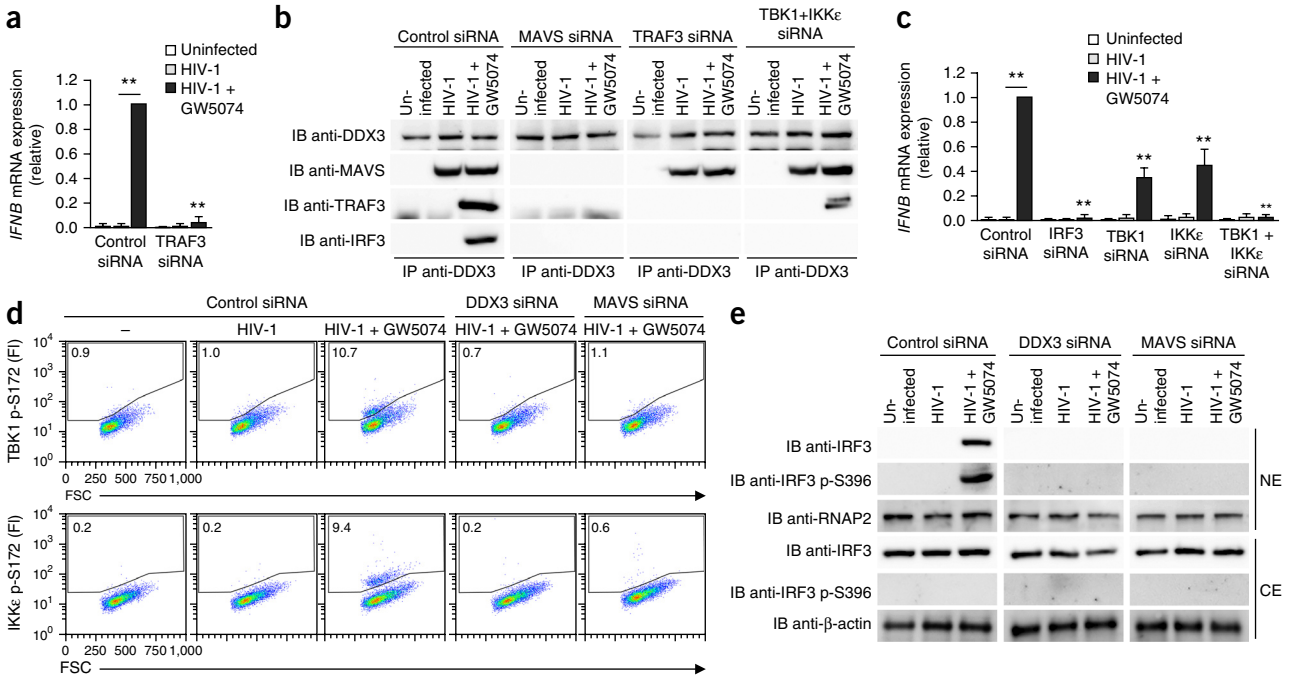

Figure 4 HIV-1 infection blocks TRAF3 recruitment to MAVS and subsequent IRF3 activation. (**a**) RT–PCR analyses of *IFNB* mRNA in moDCs 4 h after HIV-1_{BaL} infection, in the absence or presence of the Raf-1 inhibitor GW5074, and after silencing (siRNA) of TRAF3. (**b**) Immunoblot (IB) analyses of DDX3, MAVS, TRAF3 and IRF3 after IP of DDX3 from moDCs 3 h after HIV-1_{BaL} infection, in the absence or presence of GW5074, and after silencing of MAVS, TRAF3 or TKB1–IKKε expression. (**c**) RT–PCR analyses of *IFNB* mRNA in moDCs 4 h after HIV-1_{BaL} infection as in a, with silencing of TBK1, IKKε or IRF3 expression. (**d**) Flow cytometry analyses of Ser172 phosphorylation on TBK1 and IKKε in moDCs 3 h after HIV-1_{BaL} infection, in the absence or presence of GW5074, and after silencing of DDX3 or MAVS expression. FI, fluorescence intensity; FSC, forward scatter. (**e**) Immunoblot analyses of IRF3 and phosphorylated IRF3 in cytoplasmic (CE) and nuclear (NE) extracts from moDCs 3 h after HIV-1_{BaL} infection, in the absence or presence of GW5074, and after silencing of DDX3 or MAVS expression. β-actin and RNA polymerase II (RNAP2) served as loading controls. Data are representative of three independent experiments (**b**,**d**,**e**) or are the mean ± s.d. of ten (**a**) or four (**c**) different donors. $^{**}P < 0.01$ (Student's *t*-test).

MAVS expression (**Fig. 3d**). Activation of DC-SIGN using cross-linking antibodies abrogated *IFNB* expression in cap-TAR-transfected moDCs, whereas GW5074 treatment restored these responses (**Fig. 3e**). Notably, transfection of moDCs with *tat* transcripts lacking their 3′ poly(A) tail (cap-Tat) but not intact transcripts (cap-Tat-poly(A)) induced *IFNB* expression, which was abrogated by the silencing of DDX3 or MAVS expression (**Fig. 3f**). DDX3 also binds some endogenous transcripts, such as *HBB*[16] (which encodes β-globin). Transfection of moDCs with *HBB* transcripts lacking their 3′ poly(A) tail (cap-β-globin) but not with intact *HBB* transcripts (cap-β-globin-poly(A)) induced *IFNB* expression, which was abrogated by the silencing of DDX3 or MAVS expression (**Fig. 3f**). These results suggested that RNAs that bind DDX3 and avoid ribosomal recruitment induce MAVS signaling, independently of the (viral) nature of the RNA.

We next generated 293T cell lines that were depleted of either DDX3 (293TΔDDX3) or MAVS (293TΔMAVS) using CRISPR–Cas9-directed genome editing (**Supplementary Fig. 3**). Transfection of control 293T, 293TΔRIG-I, 293TΔMDA5 and 293TΔRIG-I-MDA5 cells, but not of 293TΔDDX3 or 293TΔMAVS cells, with cap-TAR RNA induced *IFNB* expression (**Fig. 3g**). The RIG-I–MDA5 ligand poly(I:C)-LyoVec induced *IFNB* expression in control 293T and 293TΔDDX3 cells but did not do so in 293TΔRIG-I, 293TΔMDA5, 293TΔRIG-I-MDA5 or 293TΔMAVS cells (**Fig. 3g**). Thus, the DDX3–MAVS sensing mechanism is not restricted to DCs and macrophages.

DDX3 activates IRF3 via TRAF3 recruitment to MAVS

RIG-I and MDA5 induce recruitment of the adaptor TRAF3 to MAVS aggregates, resulting in the subsequent activation of the IκB-kinase-related kinases TBK1 and IKKε for phosphorylation of the transcription factor IRF3 (refs. 18,23). We observed that *TRAF3* silencing by RNAi abrogated *IFNB* expression in GW5074-treated HIV-1_{BaL}-infected moDCs (**Fig. 4a**). TRAF3 co-immunoprecipitated with DDX3 from whole-cell extracts of GW5074-treated but not untreated HIV-1_{BaL}-infected moDCs, and this was abrogated by silencing of MAVS expression (**Fig. 4b**). These results implied that Raf-1 suppresses HIV-1-induced type I interferon responses by impeding recruitment of TRAF3 to MAVS.

Silencing the expression of IRF3 or of both TBK1 and IKKε by RNAi abrogated *IFNB* expression in GW5074-treated HIV-1_{BaL}-infected moDCs (**Fig. 4c**). FACS analyses showed that HIV-1_{BaL} infection of GW5074-treated moDCs induced phosphorylation of TBK1 and IKKε at Ser172, a mark of activation[24] and that this was abrogated by silencing of DDX3 or MAVS expression by RNAi (**Fig. 4d**). TBK1 and IKKε phosphorylation was only observed in approximately 10% of GW5074-treated moDCs (**Fig. 4d**), suggesting that these kinases were only activated in productively infected cells. MAVS phosphorylation by TBK1–IKKε recruits IRF3 to MAVS, which precedes the phosphorylation of IRF3 on Ser396 by TBK1–IKKε[25]. Nuclear translocation and phosphorylation of IRF3 in GW5074-treated HIV-1_{BaL}-infected moDCs was abrogated by silencing of DDX3 or MAVS expression (**Fig. 4e**). Recruitment of IRF3 to DDX3, as assessed by co-immunoprecipitation from whole-cell extracts of GW5074-treated HIV-1_{BaL}-infected moDCs, was attenuated by silencing of MAVS, TRAF3 and TBK1–IKKε expression (**Fig. 4b**). These results indicated that, after inhibition of Raf-1 activity, sensing of abortive HIV-1 RNA by DDX3 leads to MAVS–TRAF3- and TBK1–IKKε-dependent activation of IRF3.

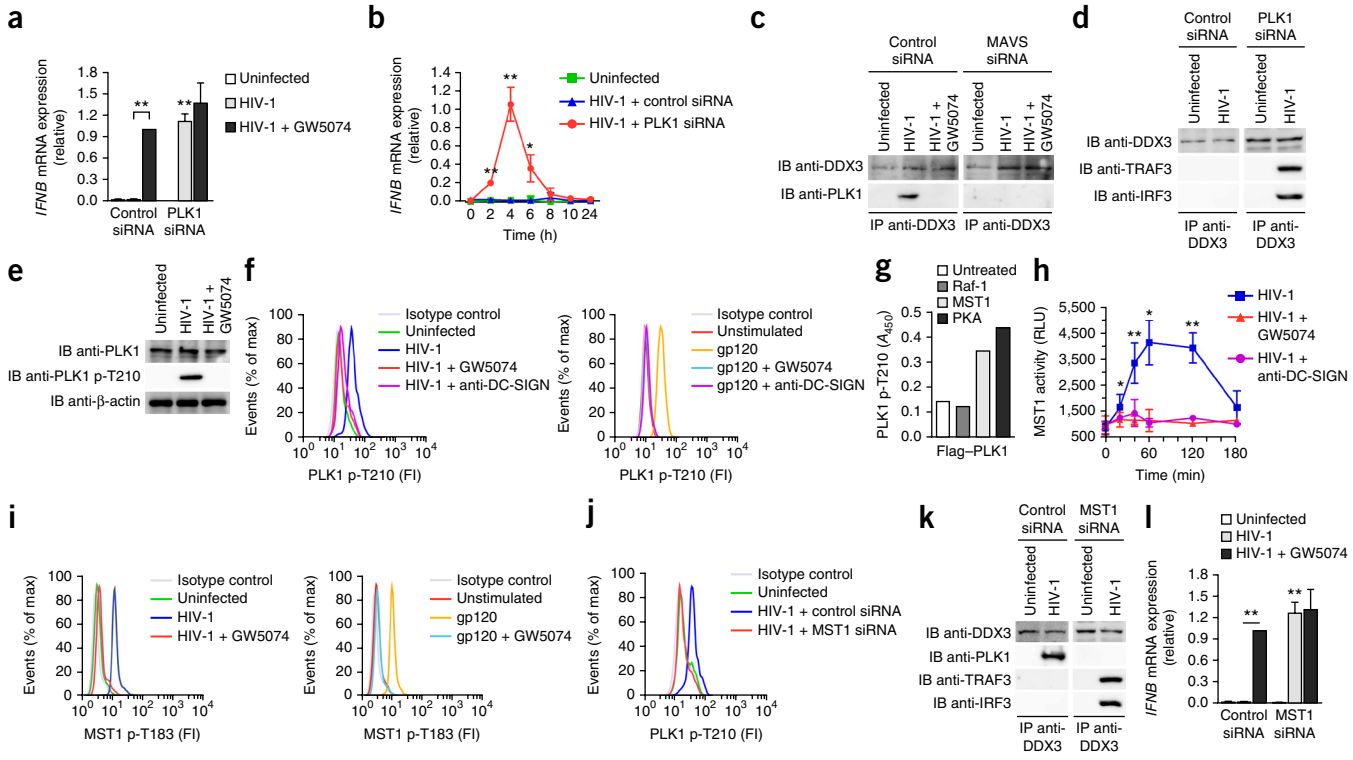

Figure 5 PLK1 activation during HIV-1 infection impedes TRAF3 recruitment to DDX3–MAVS and type I interferon responses. (**a**,**b**) RT–PCR analyses of *IFNB* mRNA in moDCs after HIV-1_{BaL} infection (4 h), in the absence or presence of GW5074 (**a**), and after silencing (siRNA) of *PLK1* (**a**,**b**). (**c**,**d**) Immunoblot (IB) analyses of DDX3, MAVS and PLK1 (**c**) or TRAF3 (**d**) after IP of DDX3 from moDCs 3 h after HIV-1_{BaL} infection, in the absence or presence of GW5074 (**c**), and after silencing of MAVS (**c**) or PLK1 (**d**) expression. (**e**,**f**) Immunoblot (**e**) and flow cytometry (**f**) analyses of Thr210 phosphorylation of PLK1 in moDCs 3 h after HIV-1_{BaL} infection or gp120 stimulation (**f**), in the absence or presence of GW5074 (**e**,**f**) or DC-SIGN-specific blocking antibodies (**f**). β-actin served as loading control (**e**). (**g**) ELISA for quantification of phosphorylation of Thr210 on Flag–PLK1 by recombinant kinases. (**h**,**i**) Kinase activity assay for MST1 activity (**h**) or flow cytometry analyses of Thr183 autophosphorylation of MST1 (**i**) in moDCs after HIV-1_{BaL} infection or gp120 stimulation (1 h), in the absence or presence of GW5074 (**h**,**i**) or DC-SIGN-specific blocking antibodies (**h**). (**j**) Flow cytometry analyses of Thr210 phosphorylation of PLK1 as in **e**,**f**, except after silencing of MST1 expression. (**k**) Immunoblot analyses of DDX3, MAVS, PLK1 and TRAF3 after IP of DDX3 from moDCs 3 h after HIV-1_{BaL} infection after silencing of MST1 expression. (**l**) RT–PCR analyses of *IFNB* mRNA in moDCs after HIV-1_{BaL} infection (4 h), in the absence or presence of GW5074, and after silencing of MST1 expression. Data are representative of three (**c**,**d**,**k**), two (**e**,**i**), six (**f**, HIV-1), four (**f**, gp120) or five (**j**) independent experiments or are the mean ± s.d. of six (**a**,**l**) or four (**b**,**h**) different donors or of three independent measurements (**g**). $*P < 0.05$ and $**P < 0.01$ (Student's *t*-test).

HIV-1-activated PLK1 impedes TRAF3 recruitment to MAVS

Association of the mitotic kinase PLK1 with MAVS blocks MAVS–TRAF3 interactions[25]. Notably, *PLK1* silencing by RNAi induced transient *IFNB* expression in untreated HIV-1_{BaL}-infected moDCs (**Fig. 5a**,**b**), similar to that observed in GW5074-treated moDCs (**Fig. 1a**,**b**). *PLK1* silencing in HIV-1_{BaL}-infected moDCs did not abrogate the induction of *tat–rev* mRNA expression (**Supplementary Fig. 4**), indicating that PLK1, unlike Raf-1, is not involved in HIV-1 transcription elongation[12]. PLK1 co-immunoprecipitated with DDX3 from whole-cell extracts of HIV-1_{BaL}-infected, but not uninfected, moDCs, and this was abrogated by *MAVS* silencing and GW5074 treatment (**Fig. 5c**). Both TRAF3 and IRF3 co-immunoprecipitated with DDX3 in *PLK1*-silenced HIV-1_{BaL}-infected moDCs (**Fig. 5d** and **Supplementary Fig. 5**). These results indicated that Raf-1 activation induces association of PLK1 with MAVS in HIV-1-infected DCs, which prevents downstream DDX3–MAVS signaling.

PLK1 resides in an inactive state due to intramolecular interactions, which are released when PLK1 becomes phosphorylated at Thr210, enabling PLK1 to bind its substrates, such as MAVS[26,27]. FACS analyses showed that both HIV-1_{BaL} infection and gp120 stimulation of moDCs induced PLK1 phosphorylation at Thr210 and that this was abrogated in the presence of blocking antibodies specific for DC-SIGN or by treatment with GW5074 (**Fig. 5e,f**), indicating that HIV-1_{BaL} induces activation of Raf-1 and subsequent phosphorylation of PLK1(Thr210) via DC-SIGN.

Recombinant Raf-1, in contrast to recombinant protein kinase A (which was used as a control), did not phosphorylate Thr210 on Flag-tagged PLK1 in a biochemical assay (**Fig. 5g**), suggesting that PLK1 is not a direct target of Raf-1. Ste20-like kinases have been reported to phosphorylate PLK1 at Thr210 (ref. 28). Because the Ste20-like kinase MST1 interacts with the adaptor protein CNK1 (ref. 29), a component of the Raf-1 signalosome that is attached to DC-SIGN in resting DCs[10], we assessed whether PLK1 is a target of MST1. Recombinant MST1 phosphorylated Flag–PLK1 at Thr210 in a biochemical assay (**Fig. 5g**). We furthermore observed transient activation of MST1 in whole-cell extracts from HIV-1_{BaL}-infected moDCs, which was abrogated by treatment with blocking antibodies specific for DC-SIGN or with GW5074 in a kinase activity assay (**Fig. 5h**). GW5074-sensitive MST1 activity after HIV-1_{BaL} infection or gp120 stimulation in moDCs coincided with MST1 phosphorylation at its autophosphorylation site Thr183 (ref. 30), as assessed by FACS analyses (**Fig. 5i**). *MST1* silencing by RNAi in HIV-1_{BaL}-infected moDCs abrogated both PLK1 phosphorylation (**Fig. 5j**) and co-immunoprecipitation of PLK1 with DDX3 from whole-cell extracts (**Fig. 5k**) while inducing TRAF3 and

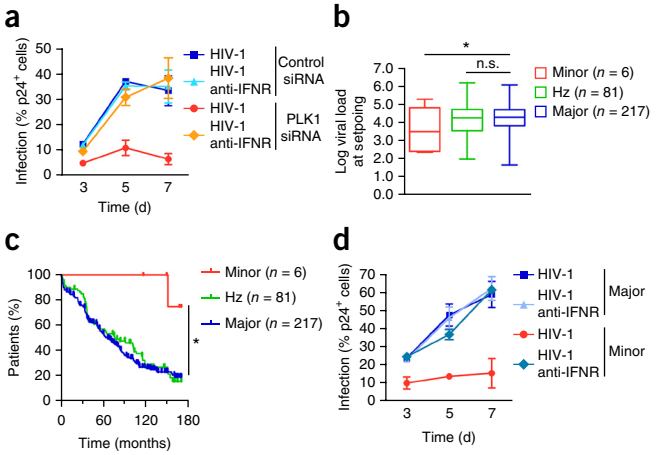

Figure 6 Type I interferon responses by DCs suppress HIV-1 replication in infected individuals. (**a**) Flow cytometry analyses of viral p24 expression in moDCs (percentage p24$^+$ cells) at 3, 5 and 7 d after HIV-1_{BaL} infection, in the absence or presence of IFNR-specific blocking antibodies, and after silencing (siRNA) of PLK1 expression. (**b**) HIV-1 RNA levels (log_{10} viral copies/ml plasma) at set point in untreated HIV-1-infected individuals in a human MSM cohort, differentiated based on genotype of linked *MAVS* SNPs rs7262903 and rs7269320 (minor, homozygous for minor alleles; Hz, heterozygous for both alleles; major, homozygous for major alleles). (**c**) Kaplan–Meier survival curve comparing the time required for log_{10} viral copies/ml plasma to reach >4.5 from time of seroconversion in untreated HIV-1-infected individuals in a human MSM cohort, differentiated by genotype as in **b**. (**d**) Flow cytometry analyses of viral p24 expression in moDCs, as in **a**, in moDCs expressing either wild-type MAVS (major genotype: homozygous for major alleles of rs7262903 and rs7269320) or MAVS(Q198K,S409F) (minor genotype). Data are representative of four (**a**), five (**d**, major) or three (**d**, minor) independent experiments (mean ± s.d. of duplicates (**a**,**d**) or of $n = 304$ patients (**b**,**c**)). $P = 0.044$, n.s., not significant ($P = 0.215$) (unpaired Student's *t*-test) (**b**); $P = 0.025$; hazard ratio (RH) = 0.106, 95% confidence interval 0.015–0.759 (Cox regression model) (**c**).

IRF3 co-immunoprecipitation with DDX3 (**Fig. 5k**), IRF3 activation (**Supplementary Fig. 5**) and *IFNB* expression (**Fig. 5l**). Similar to that seen with Raf-1 inhibition, *MST1* silencing blocked *tat–rev* mRNA expression in HIV-1_{BaL}-infected moDCs (**Supplementary Fig. 1**), suggesting that MST1 is involved in HIV-1 transcription elongation. Taken together, these data indicated that HIV-1 binding to DC-SIGN triggers Raf-1-dependent MST1 activation, which leads to PLK1 phosphorylation and subsequent PLK1 binding to MAVS, thus blocking DDX3–MAVS signaling.

Type I interferon responses suppress HIV-1 replication

We next investigated the effect of type I interferon responses on HIV-1 replication in moDCs. FACS analyses showed that blocking antibodies for the IFN-α/β receptor (IFNR) did not affect the percentage of moDCs that expressed the viral protein p24 after HIV-1_{BaL} infection (**Fig. 6a**). Silencing of PLK1 expression by RNAi lowered the percentage of p24$^+$ moDCs after HIV-1_{BaL} infection, whereas treatment with blocking antibodies to IFNR enhanced infection to levels similar to that in moDCs that were treated with a control small interfering RNA (siRNA) (**Fig. 6a**), indicating that HIV-1 requires PLK1-mediated suppression of IFN-β to efficiently infect moDCs.

We next analyzed the effect of single-nucleotide polymorphisms (SNPs) in genes encoding components of the DDX3–MAVS signaling pathway within a cohort of untreated HIV-1-infected 'men who have sex with men' (MSM cohort). We identified three SNPs within *MAVS*—rs7262903, rs7269320 and rs7267297—that showed significant differences in plasma viral load. rs7262903 and rs7269320 results in amino acid substitutions within MAVS (Gln198Lys (Q198K) and Ser409Phe (S409F), respectively), whereas rs7267297 is located within the sequence that encodes the 3′ untranslated region (UTR) of the *MAVS* mRNA. rs7262903 and rs7269320 are 100% linked within the MSM cohort ($n = 6$); linkage disequilibrium in the global population is D′ = 0.956, $r^2 = 0.559$ (HapMap release 23). Notably, plasma viral load at set point was significantly lower in HIV-1-infected individuals homozygous for the minor alleles of rs7262903 and rs7269320 (minor genotype) than in individuals homozygous for the major alleles (major genotype) (**Fig. 6b**), whereas no differences were detected in the plasma viral loads at set point between individuals with heterozygous and major genotypes (**Fig. 6b**). We observed a significant delay in the time from seroconversion to viral RNA load >$10^{4.5}$ copies/ml plasma, which was the median HIV-1 RNA load in the cohort[31], in individuals with the minor genotype than in those with the major genotype (**Fig. 6c**). There was no significant effect on disease progression (AIDS, according to the US Centers for Disease Control definition, 1993) over the course of 180 months in individuals with the minor genotype, probably because of the low number of individuals with this genotype (6/304) within the MSM cohort (data not shown). These data indicated that the DDX3–MAVS pathway was important in controlling HIV-1 replication, not only during the acute infection stage but also in the clinical latency stage.

We next examined the effect of the MAVS(Q198K,S409F) protein, which is encoded by minor genotype alleles, on HIV-1 replication in DCs from healthy donors. We observed a lower percentage of p24$^+$ moDCs derived from healthy individuals with the minor genotype (minor genotype moDCs) after HIV-1_{BaL} infection than in those from individuals with the major genotype (major genotype moDCs), whereas treatment with IFNR-specific blocking antibodies enhanced infection to levels similar to those observed in major genotype moDCs (**Fig. 6d**), indicating that suppression of type I interferon responses was defective in HIV-1-infected DCs expressing MAVS(Q198K,S409F).

Both major and minor genotype moDCs responded similarly to RIG-I–MDA5 ligands, such as poly(I:C)-LyoVec or the measles virus, for the induction of *IFNB* expression (**Fig. 7a**), indicating that MAVS(Q198K,S409F) is functionally neutral, as reported for MAVS(Q198K)[32]. HIV-1_{BaL} infection induced *IFNB* and ISG expression in both untreated and GW5074-treated minor genotype moDCs (**Fig. 7b,c**), in contrast to that observed in heterozygous genotype moDCs, which induced only *IFNB* expression after GW5074 treatment (**Fig. 7b**), similar to that observed in major genotype moDCs (**Fig. 1a**). We also observed *IFNB* expression after HIV-1_{BaL} infection of both untreated and GW5074-treated primary dermal DCs isolated from healthy minor genotype individuals (**Fig. 7d**). *IFNB* expression in HIV-1_{BaL}-infected minor genotype moDCs was abrogated by silencing of DDX3 or MAVS expression (**Fig. 7e**). Transfection of a plasmid expressing wild-type MAVS in *MAVS*-silenced minor genotype moDCs rescued *IFNB* responses that were induced by HIV-1_{BaL} infection only after GW5074 treatment (**Supplementary Fig. 6**), mimicking the responses in major genotype moDCs and indicating that the identified *MAVS* SNPs mediate the observed effects. DDX3 co-immunoprecipitated with MAVS and TRAF3, but not with PLK1, in whole-cell extracts from HIV-1_{BaL}-infected minor genotype moDCs (**Fig. 7f**). Also, *PLK1* silencing by RNAi did not affect *IFNB* expression in HIV-1_{BaL}-infected minor genotype moDCs (**Fig. 7g**). FACS analyses showed that Thr210 phosphorylation on PLK1 was normally induced by HIV-1_{BaL} infection in minor genotype moDCs (**Fig. 7h**). However, Thr210-phosphorylated Flag–PLK1 immunoprecipitated

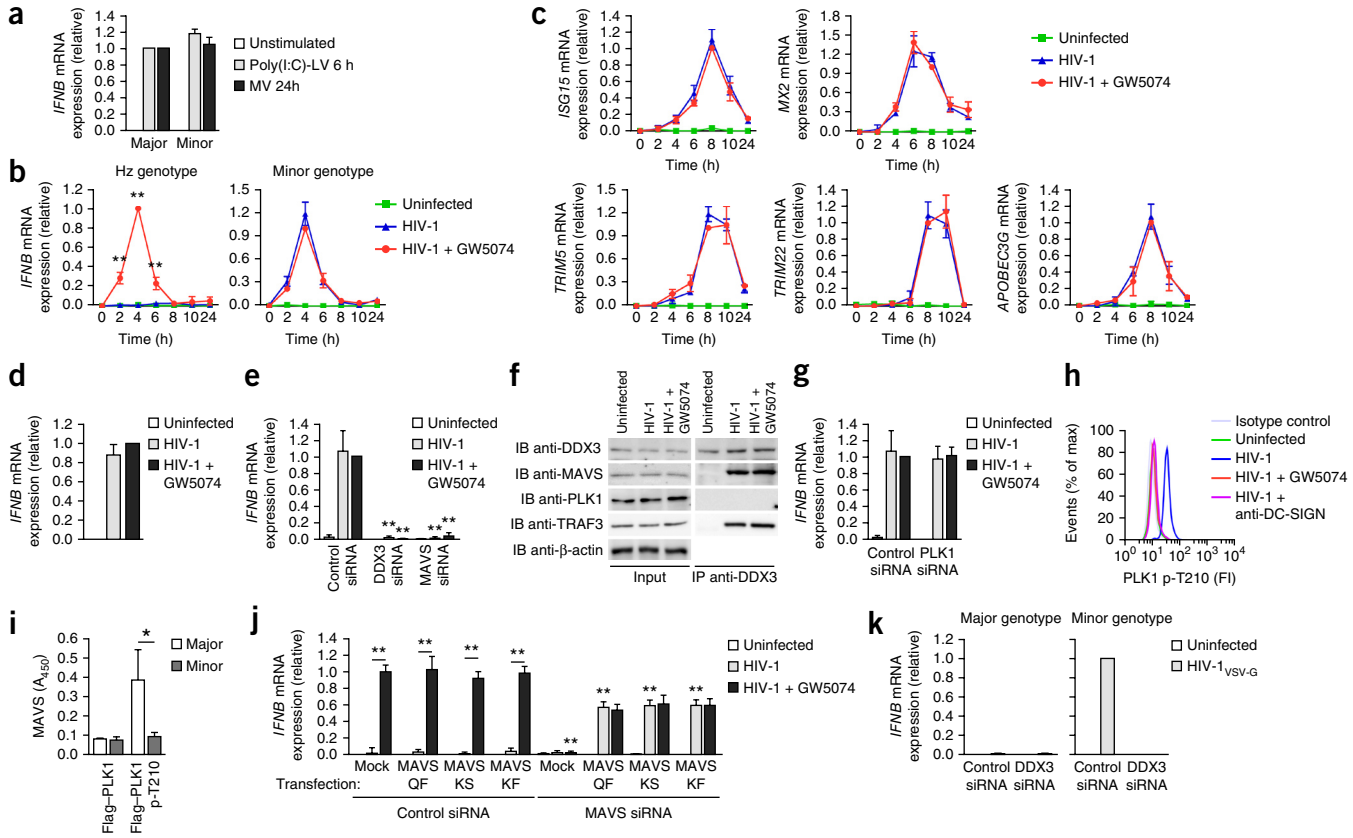

Figure 7 PLK1-mediated suppression of DDX3 signaling after HIV-1 infection is impeded by mutation of MAVS. (**a**) RT–PCR analyses of *IFNB* mRNA in moDCs with either major or minor genotype for *MAVS* SNPs rs7262903 and rs7269320 6 h after transfection with poly(I-C)-LyoVec, 24 h after infection with measles virus (MV). (**b**–**e**) RT–PCR analyses of *IFNB* (**b**,**d**,**e**) and of *ISG15*, *MX2*, *TRIM5*, *TRIM22* and *APOBEC3G* (**c**) mRNA in moDCs (**b**,**c**,**e**) or primary dermal DCs (**d**) with either heterozygous (Hz) (**b**) or minor genotypes (**b**–**e**), after HIV-1_{BaL} infection (4 h in **d**,**e**), in the absence or presence of GW5074, and after silencing of DDX3 or MAVS expression (**e**). (**f**) Immunoblot (IB) analyses for the indicated proteins after IP of DDX3 from minor genotype moDCs 3 h after HIV-1_{BaL} infection, in the absence or presence of GW5074. β-actin served as loading control. (**g**) RT–PCR analyses of *IFNB* mRNA in minor genotype moDCs, in the absence or presence of GW5074, and after silencing of PLK1 expression. (**h**) Flow cytometry analyses of Thr210 phosphorylation on PLK1 in minor genotype moDCs 3 h after HIV-1_{BaL} infection, in the absence or presence of GW5074 or DC-SIGN-specific blocking antibodies. (**i**) ELISA of association between Thr210-phosphorylated Flag–PLK1 and MAVS in lysates from either major or minor genotype moDCs. (**j**) RT–PCR analyses of *IFNB* mRNA in MAVS-silenced moDCs 4 h after HIV-1_{BaL} infection, in the absence or presence of GW5074, after complementation of MAVS expression by transfection of plasmids expressing RNAi-resistant cDNAs encoding single (QF, Q198,S409F; KS, Q198K,S409) or double (KF, Q198K,S409F) amino acid substitutions in MAVS. (**k**) RT–PCR analyses of *IFNB* mRNA in moDCs with either the major or minor genotype for *MAVS* SNPs rs7262903 and rs7269320 4 h after infection with HIV-1_{VSV-G}, after silencing of DDX3 expression. Data are representative of three independent experiments (**f**–**h**) or are the mean ± s.d. of two (**d**, minor genotype; **k**), three (**a**;**b**, minor genotype; **c**;**e**;**g**;**i**) or four (**b**, Hz genotype; **j**) different donors. $^*P < 0.05$ and $^{**}P < 0.01$ (unpaired Student's *t*-test (**i**) or Student's *t*-test (**j**)).

MAVS from lysates of major genotype moDCS but not minor genotype moDCs (**Fig. 7i**). We next investigated whether either Q198K or S409F or both mutations in MAVS were required to block PLK1–MAVS interactions. HIV-1_{BaL} infection induced *IFNB* expression in *MAVS*-silenced moDCs that were complemented with plasmids expressing MAVS(Q198K), MAVS(S409F) or MAVS(Q198K,S409F), in contrast to the control-siRNA-silenced moDCs that still expressed wild-type MAVS (**Fig. 7j**), indicating that both mutations are required for PLK1-mediated MAVS suppression.

Similar to infection with HIV-1_{BaL}, infection of moDCs with vesicular stomatitis virus (VSV)-G-pseudotyped HIV-1 (HIV-1_{VSV-G}) does not result in type I interferon responses[33,34]. During HIV-1_{VSV-G} infection, retroviral integration and transcriptional initiation occur in a similar time frame as that observed for HIV-1_{BaL}; however, the VSV-G envelope does not bind DC-SIGN[12]. Infection of minor genotype moDCS but not major genotype moDCs with HIV-1_{VSV-G} induced *IFNB* expression 4 h after infection, and this was abrogated by silencing of DDX3 expression (**Fig. 7k**), indicating that HIV-1_{VSV-G}induces inhibition of MAVS signaling independently of DC-SIGN. Thus, both HIV-1 and VSV-G target MAVS for suppression of IFN-β expression.

Attenuation of DDX3–MAVS signaling suppresses immune activation

We next addressed whether suppression of DDX3–MAVS signaling prevented DC activation in response to HIV-1 infection. We only observed enhanced expression of the maturation markers CD80, CD83 and CD86 in GW5074-treated but not in untreated HIV-1_{BaL}-infected moDCs by FACS analyses, which was abrogated by treatment with IFNR-specific blocking antibodies or by silencing of DDX3 or MAVS expression by RNAi (**Fig. 8a**,**b**). In contrast, HIV-1_{BaL} infection of *PLK1*-silenced or minor genotype moDCs induced expression of these maturation markers even without GW5074 treatment, which was inhibited by treatment with the IFNR-specific blocking antibodies (**Fig. 8a**,**b**). These data strongly indicated that type I interferon responses are essential for DC maturation. Thus, HIV-1 targets DDX3–MAVS signaling not only to block antiviral responses but to block adaptive immune responses as well (**Supplementary Fig. 7**).

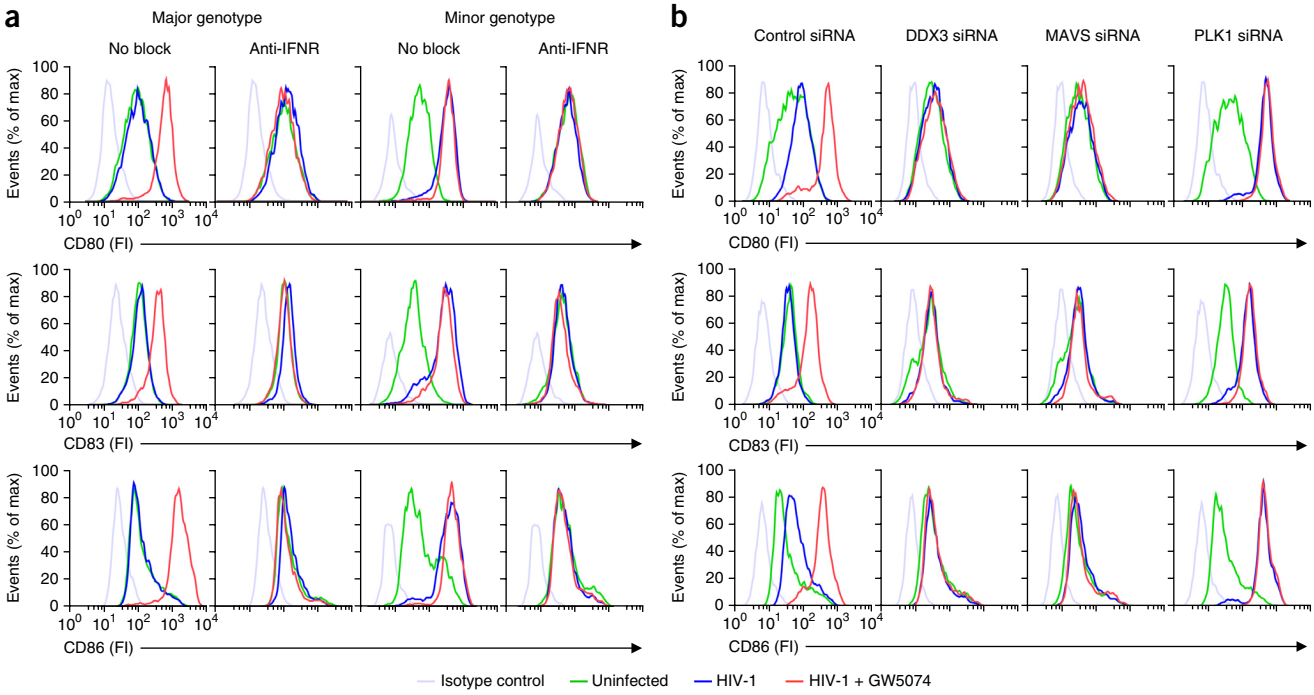

Figure 8 HIV-1 infection attenuates DDX3–MAVS-mediated DC maturation. (**a**,**b**) Flow cytometry analyses for the expression of the maturation markers CD80, CD83 and CD86 on moDCs with either major (**a**,**b**) or minor (**a**) rs7262903 and rs7269320 genotypes, 48 h after HIV-1_{BaL} infection, in the absence or presence of GW5074, with or without treatment with IFNR-specific blocking antibodies (**a**), and after silencing of DDX3, MAVS or PLK1 expression (**b**). FI, fluorescence intensity. Data are representative of five (**a**, major genotype), three (**a**, minor genotype) or six (**b**) independent experiments.

DISCUSSION

HIV-1 avoids immune surveillance required for the mounting of protective responses. Here we identified the RNA helicase DDX3 as an intracellular sensor that coupled recognition of abortive HIV-1 RNA to the induction of antiviral responses. DDX3 is ideally suited as a HIV-1 RNA sensor, as it is also essential for HIV-1 replication by facilitating nuclear export[14] and translation[16,17] of HIV-1 transcripts. All HIV-1 transcripts—spliced, unspliced, abortive or full-length—share the same highly structured ~58 nt of the 5′ UTR[13] and interact with DDX3. DDX3 bound to abortive HIV-1 RNAs did not assemble in translation complexes, as these abortive RNAs lack a poly(A) tail, which prevents PABP binding. Instead, the DDX3-abortive RNA complexes associated with MAVS, which led to antiviral responses. The roles of DDX3 in HIV-1 translation and antiviral defense are thus mutually exclusive, which might prevent triggering of antiviral immune responses to endogenous transcripts that also interact with DDX3 (ref. 16).

Abortive HIV-1 RNAs are generated early after integration[12], and therefore, DDX3-mediated type I interferon responses were induced very rapidly, within 4 h after infection, as opposed to antiviral responses to VSV-G-pseudotyped HIV-1, which are detected 22 h after infection of Vpx-treated DCs[34]. Abortive HIV-1 RNAs are also found in high amounts in latently infected cells[35], and it will be interesting to examine whether they can induce type I interferon responses via DDX3.

HIV-1 infection blocked DDX3 signaling at the level of TRAF3 recruitment to MAVS via DC-SIGN-dependent activation of PLK1. Our data underline the importance of host innate receptors for HIV-1 in suppressing antiviral host defenses and show the parallel existence of various HIV-1-sensing mechanisms in DCs that are restricted in different ways[36]: while cGAS signaling after sensing of cDNA is blocked by the presence of the host exonuclease TREX1 (ref. 20), signaling by DDX3 after sensing of abortive transcription products was blocked by simultaneous activation of the host factor PLK1 via DC-SIGN after HIV-1 infection. Our data also showed that viral blocking of type I interferon responses by interference at the level of MAVS was not limited to DC-SIGN signaling, as VSV-G-pseudotyped HIV-1 also inhibited MAVS signaling, even though the VSV-G envelope does not engage DC-SIGN. MAVS targeting or PLK1 activation might be a versatile tool for different viruses to evade immune responses. PLK1 activation can be achieved by a variety of kinases, mostly by members of the broad family of Ste20-related serine–threonine kinases[28], and PLK1 activation by HIV-1_{VSV-G} might be achieved by tumor necrosis factor, which is induced after infection with HIV-1_{VSV-G}, but not with HIV-1 (ref. 12). These observations also signify that the interpretation of experiments using VSV-G-pseudotyped viruses or particles should take into account the distinct effects of the VSV-G envelope.

PLK1 has a critical role in cell division; however, its role in nondividing, differentiated cells is poorly defined[37]. Our data identified PLK1 as an inhibitor of antiviral defense against HIV-1 in DCs. Although PLK1 association with MAVS blocked recruitment of TRAF3 to MAVS, the exact underlying mechanism remains to be elucidated. PLK1 could block aggregation of MAVS, which is a prerequisite for downstream signaling by MAVS for IRF3 activation[23]. Our data suggest that PLK1 inhibitors[38] could constitute a novel class of antiretroviral drugs that enhances endogenous antiviral immunity in individuals potentially infected with HIV-1.

The importance of early type I interferon responses in HIV-1 infection was substantiated by the identification of two linked SNPs within the *MAVS* gene that encode a double mutant, MAVS(Q198K,S409F). Our data showed that this double mutant was insensitive to PLK1 suppression and could thereby orchestrate

an effective antiviral defense after HIV-1 infection via the induction of DC maturation and a type I interferon response. Notably, we observed that markedly prolonged suppression of plasma viral load in individuals infected with HIV-1 in a human MSM HIV-1 infection cohort was associated with homozygosity for the rare *MAVS* allele that encodes this double mutant. The exact consequences of type I interferon responses during HIV-1 infection are a topic of debate. Inflammation during infection is predictive of non-AIDS morbidity and death, as well as high set point plasma virus load[39,40]. Type I interferon responses are especially important in limiting viral spread; however, during HIV-1 infection, they might also result in more T cell activation and therefore more HIV-1 target cells[41,42]. Inhibition of type I interferon responses in nonhuman primates early during SIV infection decreases the expression of genes involved in antiviral responses, increases the SIV reservoir size and results in faster T cell depletion with progression to AIDS, whereas continuous exposure to type I interferon leads to desensitization and increases disease progression[8]. Our data in untreated patients with HIV-1 who express MAVS(Q198K,S409F) corroborated that early antiviral responses during infection are beneficial in host control of viral replication also during the clinical latency stage. Localized vaginal application of type I interferon shortly before HIV-1 exposure decreases viral replication in humanized mice[43]. Our observation that inhibition of the DDX3–MAVS blockade in primary human vaginal DCs after HIV-1 infection restored type I interferon responses would suggest that topical therapeutic targeting could be beneficial during the process of sexual transmission of the virus. Overall, our study underscores the importance of antiviral type I interferon responses in acute retroviral exposure, during which time DCs are a prominent target for HIV-1, which is also required to limit viral replication at the clinical latency stage, and reveals the identified pathways as important novel targets for early therapeutic intervention to boost endogenous antiviral immunity in acute exposure or even as a prophylactic measure.

METHODS

Methods, including statements of data availability and any associated accession codes and references, are available in the online version of the paper.

Note: Any Supplementary Information and Source Data files are available in the online version of the paper.

ACKNOWLEDGMENTS

We thank L. Westera, C. Buskens and W. Bemelman (AMC, Amsterdam, the Netherlands) for the intestinal tissue cell suspensions and C.L. Verweij (VUmc, Amsterdam, the Netherlands) for the *IFNB*, *ISG15* and Mx2 primer sequences. HIV-2 virus, MT-2 cells, AZT and gp120 were obtained through the NIH AIDS Research and Reference Reagent Program. Supported by Aids Fonds (2012042; S.I.G.), the Netherlands Organization for Scientific Research (NWO) VICI 918.10.619; T.B.H.G.) and the European Research Council (Advanced grant 670424; T.B.H.G.).

AUTHOR CONTRIBUTIONS

S.I.G. designed and supervised research, and performed experiments; N.H., T.M.K., E.M.Z.-W., R.S.-F., J.K.S., N.H.v.T., C.M.S.R. and A.D. performed experiments; N.H. generated the 293T CRISPR knockout cell lines; N.A.K. and T.B. provided data from the Amsterdam cohort studies (ACS) on HIV-1 infection and AIDS; K.A.v.D. assisted with virus isolation; and S.I.G. and T.B.H.G. interpreted results and wrote the paper.

COMPETING FINANCIAL INTERESTS

The authors declare no competing financial interests.

1. Steinman, R.M. Decisions about dendritic cells: past, present, and future. *Annu. Rev. Immunol.* **30**, 1–22 (2012).
2. Miller, E. & Bhardwaj, N. Dendritic cell dysregulation during HIV-1 infection. *Immunol. Rev.* **254**, 170–189 (2013).
3. Goujon, C. *et al.* Human MX2 is an interferon-induced post-entry inhibitor of HIV-1 infection. *Nature* **502**, 559–562 (2013).
4. Kane, M. *et al.* MX2 is an interferon-induced inhibitor of HIV-1 infection. *Nature* **502**, 563–566 (2013).
5. Yan, N. & Chen, Z.J. Intrinsic antiviral immunity. *Nat. Immunol.* **13**, 214–222 (2012).
6. Simmons, D.P. *et al.* Type I IFN drives a distinctive dendritic cell maturation phenotype that allows continued class II MHC synthesis and antigen processing. *J. Immunol.* **188**, 3116–3126 (2012).
7. González-Navajas, J.M., Lee, J., David, M. & Raz, E. Immunomodulatory functions of type I interferons. *Nat. Rev. Immunol.* **12**, 125–135 (2012).
8. Sandler, N.G. *et al.* Type I interferon responses in rhesus macaques prevent SIV infection and slow disease progression. *Nature* **511**, 601–605 (2014).
9. Gringhuis, S.I. *et al.* C-type lectin DC-SIGN modulates Toll-like receptor signaling via Raf-1-kinase-dependent acetylation of transcription factor NF-κB. *Immunity* **26**, 605–616 (2007).
10. Gringhuis, S.I., den Dunnen, J., Litjens, M., van der Vlist, M. & Geijtenbeek, T.B.H. Carbohydrate-specific signaling through the DC-SIGN signalosome tailors immunity to *Mycobacterium tuberculosis*, HIV-1, and *Helicobacter pylori*. *Nat. Immunol.* **10**, 1081–1088 (2009).
11. Solis, M. *et al.* RIG-I-mediated antiviral signaling is inhibited in HIV-1 infection by a protease-mediated sequestration of RIG-I. *J. Virol.* **85**, 1224–1236 (2011).
12. Gringhuis, S.I. *et al.* HIV-1 exploits innate signaling by TLR8 and DC-SIGN for productive infection of dendritic cells. *Nat. Immunol.* **11**, 419–426 (2010).
13. Kao, S.Y., Calman, A.F., Luciw, P.A. & Peterlin, B.M. Anti-termination of transcription within the long terminal repeat of HIV-1 by tat gene product. *Nature* **330**, 489–493 (1987).
14. Yedavalli, V.S., Neuveut, C., Chi, Y.H., Kleiman, L. & Jeang, K.T. Requirement of DDX3 DEAD box RNA helicase for HIV-1 Rev–RRE export function. *Cell* **119**, 381–392 (2004).
15. Naji, S. *et al.* Host cell interactome of HIV-1 Rev includes RNA helicases involved in multiple facets of virus production. *Mol. Cell. Proteomics* **11**, 015313 (2012).
16. Soto-Rifo, R. *et al.* DEAD-box protein DDX3 associates with eIF4F to promote translation of selected mRNAs. *EMBO J.* **31**, 3745–3756 (2012).
17. Soto-Rifo, R., Rubilar, P.S. & Ohlmann, T. The DEAD-box helicase DDX3 substitutes for the cap-binding protein eIF4E to promote compartmentalized translation initiation of the HIV-1 genomic RNA. *Nucleic Acids Res.* **41**, 6286–6299 (2013).
18. Goubau, D., Deddouche, S. & Reis e Sousa, C. Cytosolic sensing of viruses. *Immunity* **38**, 855–869 (2013).
19. Gao, D. *et al.* Cyclic GMP–AMP synthase is an innate immune sensor of HIV and other retroviruses. *Science* **341**, 903–906 (2013).
20. Yan, N., Regalado-Magdos, A.D., Stiggelbout, B., Lee-Kirsch, M.A. & Lieberman, J. The cytosolic exonuclease TREX1 inhibits the innate immune response to human immunodeficiency virus type 1. *Nat. Immunol.* **11**, 1005–1013 (2010).
21. Lahouassa, H. *et al.* SAMHD1 restricts the replication of human immunodeficiency virus type 1 by depleting the intracellular pool of deoxynucleoside triphosphates. *Nat. Immunol.* **13**, 223–228 (2012).
22. Hertoghs, N. *et al.* SAMHD1 degradation enhances active suppression of dendritic cell maturation by HIV-1. *J. Immunol.* **194**, 4431–4437 (2015).
23. Hou, F. *et al.* MAVS forms functional prion-like aggregates to activate and propagate antiviral innate immune response. *Cell* **146**, 448–461 (2011).
24. Clark, K., Plater, L., Peggie, M. & Cohen, P. Use of the pharmacological inhibitor BX795 to study the regulation and physiological roles of TBK1 and IκB kinase epsilon: a distinct upstream kinase mediates Ser172 phosphorylation and activation. *J. Biol. Chem.* **284**, 14136–14146 (2009).
25. Saha, S.K. *et al.* Regulation of antiviral responses by a direct and specific interaction between TRAF3 and Cardif. *EMBO J.* **25**, 3257–3263 (2006).
26. Vitour, D. *et al.* Polo-like kinase 1 (PLK1) regulates interferon (IFN) induction by MAVS. *J. Biol. Chem.* **284**, 21797–21809 (2009).
27. Elia, A.E. *et al.* The molecular basis for phosphodependent substrate targeting and regulation of Plks by the Polo-box domain. *Cell* **115**, 83–95 (2003).
28. Ji, J.H. *et al.* Purification and proteomic identification of putative upstream regulators of polo-like kinase 1 from mitotic cell extracts. *FEBS Lett.* **584**, 4299–4305 (2010).
29. Rabizadeh, S. *et al.* The scaffold protein CNK1 interacts with the tumor suppressor RASSF1A and augments RASSF1A-induced cell death. *J. Biol. Chem.* **279**, 29247–29254 (2004).
30. Praskova, M., Khoklatchev, A., Ortiz-Vega, S. & Avruch, J. Regulation of the MST1 kinase by autophosphorylation, by the growth inhibitory proteins RASSF1 and NORE1, and by Ras. *Biochem. J.* **381**, 453–462 (2004).
31. de Roda Husman, A.M. *et al.* Association between CCR5 genotype and the clinical course of HIV-1 infection. *Ann. Intern. Med.* **127**, 882–890 (1997).
32. Pothlichet, J. *et al.* A loss-of-function variant of the antiviral molecule MAVS is associated with a subset of systemic lupus patients. *EMBO Mol. Med.* **3**, 142–152 (2011).
33. Pertel, T., Reinhard, C. & Luban, J. Vpx rescues HIV-1 transduction of dendritic cells from the antiviral state established by type 1 interferon. *Retrovirology* **8**, 49 (2011).

34. Manel, N. *et al.* A cryptic sensor for HIV-1 activates antiviral innate immunity in dendritic cells. *Nature* **467**, 214–217 (2010).
35. Adams, M. *et al.* Cellular latency in human-immunodeficiency-virus-infected individuals with high CD4 levels can be detected by the presence of promoter-proximal transcripts. *Proc. Natl. Acad. Sci. USA* **91**, 3862–3866 (1994).
36. Luban, J. Innate immune sensing of HIV-1 by dendritic cells. *Cell Host Microbe* **12**, 408–418 (2012).
37. Archambault, V. & Glover, D.M. Polo-like kinases: conservation and divergence in their functions and regulation. *Nat. Rev. Mol. Cell Biol.* **10**, 265–275 (2009).
38. Li, S., Zhang, Y. & Xu, W. Developments of polo-like kinase 1 (Plk1) inhibitors as anticancer agents. *Mini Rev. Med. Chem.* **13**, 2014–2025 (2013).
39. Hunt, P.W. *et al.* Gut epithelial barrier dysfunction and innate immune activation predict mortality in treated HIV infection. *J. Infect. Dis.* **210**, 1228–1238 (2014).
40. Roberts, L. *et al.* Genital tract inflammation during early HIV-1 infection predicts higher plasma viral load set point in women. *J. Infect. Dis.* **205**, 194–203 (2012).
41. Fernandez, S. *et al.* $CD4^+$ T cell deficiency in HIV patients responding to antiretroviral therapy is associated with increased expression of interferon-stimulated genes in $CD4^+$ T cells. *J. Infect. Dis.* **204**, 1927–1935 (2011).
42. Fraietta, J.A. *et al.* Type I interferon upregulates Bak and contributes to T cell loss during human immunodeficiency virus (HIV) infection. *PLoS Pathog.* **9**, e1003658 (2013).
43. Wheeler, L.A. *et al. TREX1* knockdown induces an interferon response to HIV that delays viral infection in humanized mice. *Cell Rep.* **15**, 1715–1727 (2016).

ONLINE METHODS

Dendritic cell and macrophage isolation. Monocyte-derived DCs were generated from the blood of healthy volunteer donors (Sanquin) as described[44]. Monocyte-derived macrophages were generated from isolated monocytes by culturing in RPMI medium (Gibco) with 10% FCS and 50 ng/ml macrophage colony-stimulating factor (M-CSF; Immunotools) for 7 d, while 500 U/ml IL-4 (Invitrogen) was added for the last 48 h. Primary DCs were isolated from the blood of healthy volunteer donors, skin and vaginal tissues were obtained from healthy individuals undergoing reconstructive plastic procedure or vaginal prolapse surgery, respectively, and healthy bowel tissues were from patients with cancer or those with colitis ulcerosa undergoing colectomy. Tissue harvesting procedures were approved by the AMC Medical Ethics Committee. Split-skin grafts 0.3 mm in thickness were obtained using a dermatome (Zimmer) and digested for 45 min at 37 °C with 2 μg/ml dispase II (Roche Diagnostics) to separate the dermis from the epidermis. Dermis and vaginal tissues were further treated with 5 mg/ml collagenase D and 200 U/ml DNase I (both from Roche Diagnostics) for 90 min at 37 °C after mechanical fragmentation with forceps and scissors. Mucosa from bowel tissues was separated from underlying tissues using scissors and digested with 1 mg/ml collagenase D, 50 μg/ml DNase I (both Roche diagnostics) and 1 mg/ml soybean trypsin inhibitor (Invitrogen) for 1 h at 37 °C; this was followed by mechanical dissociation using the GentleMACS Dissociator (Myltenyi Biotec). Digested tissues were then passed over a 100-μM cell strainer (Greiner) to obtain single-cell suspensions. DC-SIGN$^+$ cells were then isolated using a CD209 MicroBead kit (Miltenyi Biotec). Blood and tissue samples were routinely screened for SNPs rs7262903, rs7269320 and rs7267297 using TaqMan genotyping Assays (ID C_25623847, C_25623845, and C_29168352; Applied Biosystems); only cells with the major genotype profile for all three SNPs were used, unless otherwise stated.

293T CRISPR–Cas9 knockout cell lines. 293T cells were transfected with 2 μg CRISPR–Cas9-expressing knockout plasmids (control, sc-418922; DDX3, sc-419975; MAVS, sc-400769; RIG-I, sc-432915; MDA5, sc-401962; all from Santa Cruz) using the GeneJuice transfection reagent (Novagen) as described by the manufacturer. The knockout plasmids are a mixture of three plasmids, each carrying a different guide RNA specific for the target gene, as well as the Cas- and GFP-coding regions. GFP$^+$ cells were selected by sorting on a SH800S Cell Sorter (Sony Biotechnology) 24 to 48 h after transfection, and depletion of target proteins was verified by immunoblotting (**Supplementary Fig. 4**).

Cell treatment. Cells were stimulated with 10 ng/ml LPS from *Salmonella typhosa* (Sigma), 5 μg/ml TLR8 ligand R848, 10 μg/ml TLR2 ligand MDP, 1 μg/ml poly(I:C)-LyoVec, 1 μg/ml 3′,3′-cGAMP, 1 μg/ml herpes simplex virus (HSV) DNA–LyoVec (all from Invivogen), 10 μg/ml recombinant gp120 (NIH AIDS Research and Reference Reagent Program), or 10 μM RNA sequences corresponding to either abortive HIV-1 RNA, full-length HIV-1 *tat* transcripts or full-length transcripts encoding human β-globin that were coupled to LyoVec (Invivogen) as described by the manufacturer. The RNA sequences were produced via *in vitro* transcription (IVT) by BioSynthesis (http://www.biosyn.com); 5′ m^7GTP structures were added during IVT by co-capping, while a 3′ poly(A) tail was added by enzymatic tailing. DC-SIGN cross-linking with antibodies was performed as described[44]. Sequences are listed in **Supplementary Table 1**. Cells were infected with HIV-1, HIV-2, HTLV-1 or HIV-$1_{VSV\text{-}G}$ at MOI 0.1–0.4 (see below) or rMS^{KV} (see ref. 44) as described. Preincubation with inhibitors or blocking antibodies was done for 2 h: 1 μM GW5074 (Calbiochem), 5 μg/ml AZT (NIH AIDS Research and Reference Reagent Program), 50 nM Raltegravir (Merck), 20 μg/ml anti-DC-SIGN (AZN-D1), 20 μg/ml anti-IFNα/βR2 (MMHAR-2; PBL Interferon Source) and 20 μg/ml mouse IgG2a isotype (14-4724-85; eBioscience) as control. DCs were transfected with 25 nM siRNA using transfection reagent DF4 (Dharmacon) and used for experiments 72 h later. SMARTpool siRNAs used were: Raf-1 (M-003601-02), TLR8 (M-004715-01), TREX1 (M-013239-03), cGAS (M-015607-01), STING (M-024333-00), RIG-I (M-012511-01), MDA5 (M-013041-00), DDX1 (M-011993-00), DDX3 (M-006874-01), DDX5 (M-003774-01), MAVS (M-024237-02), TRAF3 (M-005252-02), TBK1 (M-003788-02), IKKε (M-003723-02), IRF3 (M-006875-02), PLK1 (M-003290-01) and non-targeting siRNA (D-001206-13) as a control; ON-TARGET plus siRNA used was: MST1 (L-008946-02) (all Dharmacon). Silencing of expression was verified by real-time PCR, flow cytometry and immunoblotting (**Supplementary Fig. 8** and **Supplementary Table 2**); antibodies used for verification were: anti-Raf-1 (1:500; 9422; Cell Signaling), anti-TLR8 (1:500; sc-25467; Santa Cruz), anti-RIG-I (1:1,000; 3743; Cell Signaling), anti-MDA5 (1:1,000; 4109; Cell Signaling), anti-TREX1 (1:1,000; 12215; Cell Signaling), anti-cGAS (1:1,000; 15102; Cell Signaling), anti-STING (1:1,000; 13647; Cell Signaling), anti-DDX1 (1:500; ab151962, Abcam), anti-DDX3 (1:1,000; 2635; Cell Signaling), anti-DDX5 (1:500; ab128928, Abcam), anti-MAVS (1:1,000; 3993; Cell Signaling), anti-TRAF3 (1:1,000; 4729; Cell Signaling), anti-TBK1 (1:1,000; 3504; Cell Signaling), anti-IKKε (1:1,000; 2905; Cell Signaling), anti-IRF3 (1:500; sc-9082; Santa Cruz), anti-PLK1 (1:1,000; 4513; Cell Signaling) and anti-MST1 (1:500; ab57836, Abcam), followed by incubation with either PE-conjugated anti-rabbit (1:200; 711-116-152; Jackson ImmunoResearch) or Alexa488-conjugated anti-mouse (1:400; A11029; Invitrogen) (flow cytometry), or with HRP-conjugated secondary antibody (1:2,500; 21230; Pierce) or anti-mouse (1:1,000; sc-2314; Santa Cruz) followed by ECL detection (Pierce) (immunoblotting). Rescue of DDX3 or MAVS expression after silencing was achieved by transfecting DCs for 48 h with LyoVec-coupled (see above) pcDNA3-based expression plasmids containing cDNAs with synonymous mutations that rendered them resistant to the used DDX3 and MAVS siRNAs. MAVS cDNA was further modified to encode single Q198K or S409F and dual Q198K-S409F mutants. Plasmids were generated by Life Technologies (ThermoFisher Scientific). Expression of transfected DDX3 and MAVS was verified by flow cytometry using anti-DDX3 (1:50; 2635; Cell Signaling) and anti-MAVS (1:50; 3993; Cell Signaling) (**Supplementary Fig. 6**).

MSM cohort. Untreated HIV-1-infected MSM participating in the Amsterdam cohort studies (ACS) on HIV-1 infection and AIDS (http://www.amsterdamcohortstudies.org) were genotyped and used for subsequent analyses. Treatment details and exclusion criteria have been described[45]. ACS are conducted in accordance with ethical principles set out in the declaration of Helsinki and approved by the AMC Medical Ethics Committee; all participants provided written informed consent.

Viruses and infection. HIV-1_{BaL}, HIV-1_{SF162}, HIV-1_{R9} and HIV-1_{LAI} as well as VSV-G-pseudotyped HIV-1 NL4.3-Δenv were produced and titers quantified as described[12,46]. Clinical HIV-1 isolates were produced as described[47]. HIV-2 7312A was obtained through the NIH AIDS Research and Reference Reagent Program. HTLV-1 virus was isolated from supernatant of MT-2 cells (NIH AIDS Research and Reference Reagent Program). DCs or macrophages were infected at a multiplicity of infection of 0.1–0.4; infection was determined by viral transcript (*tat-rev*, *tax-rex*[48]) quantification or flow cytometry (p24). mRNA isolation, cDNA synthesis and real-time PCR were performed as described[12]; relative mRNA expression was obtained by setting N_t ($= 2^{Ct(GAPDH) - Ct(target)}$) to 1 in 4 h-infected DCs, within one experiment and for each donor, except in time course experiments in which $N_t = 1$ at 8 h (HIV-1 Tat-Rev). Primers are listed in **Supplementary Table 2**. Intracellular p24 was detected after 3, 5 and 7 d by anti-p24 (KC57-RD1; Beckman Coulter).

Immune responses. *IFNB* and ISG mRNA levels were quantified as described above; N_t was set at 1 in 4-h (*IFNB*) or 8-h (ISGs) GW5074-treated HIV-1-infected DCs. Primers are listed in **Supplementary Table 2**. DC maturation was determined 48 h post infection by flow cytometry analysis of CD80 (557227; BD), CD83 (555658; BD) and CD86 (PN1M2218; Beckmann Coulter) cell surface expression.

Association of DDX3–MAVS–TRAF3–IRF3 and PLK1. Whole-cell extracts from HIV-1-infected DCs were prepared 3 h post infection using RIPA buffer (Cell Signaling). DDX3- or MAVS-associated proteins were immunoprecipitated from 40 μg of extract with 4 μg anti-DDX3 (sc-98711) or anti-MAVS (sc-68926; both Santa Cruz) coated on protein A/G-PLUS agarose beads (Santa Cruz). Either 20 μg of extract or immunoprecipitate was resolved by SDS–PAGE and detected by immunoblotting with anti-DDX3 (1:1,000; 2635; Cell Signaling), anti-MAVS (1:1,000; 3993; Cell Signaling), anti-TRAF3 (1:1,000; 4729; Cell Signaling), anti-IRF3 (1:500; sc-9082; Santa Cruz) or anti-PLK1 (1:1,000; 4513; Cell Signaling), followed by incubation with horseradish

doi:10.1038/ni.3647

peroxidase (HRP)-conjugated secondary antibody (1:2,500; 21230; Pierce) and ECL detection (Pierce). To ensure that equal amounts of protein were used for immunoprecipitation, membranes were also incubated with anti-β-actin (1:2,000; sc-81178; Santa Cruz), followed by HRP-conjugated anti-mouse-Ig (1:1,000; sc-2314; Santa Cruz).

Association of DDX3 with mitochondrial MAVS was visualized by confocal microscopy. DCs were infected for 3 h; during the last 30 min 200 nM MitoTracker Red CMXRos (Cell Signaling) was added to the medium. Cells were then fixed with 4% paraformaldehyde, permeabilized with 0.2% (vol/vol) Triton X-100 in PBS, and stained with anti-DDX3 (1:50; sc-98711; Santa Cruz), followed by Alexa-Fluor-488-conjugated anti-rabbit Ig (1:400; A21206; Life Technologies), together with 1 μg/ml Hoechst (Invitrogen). Visualization was done with a Leica TCS SP8 X confocal microscope.

Association of PLK1 with either wild-type or mutant MAVS was further examined by capture ELISA. 50 ng Thr210-phosphorylated Flag–PLK1 (Origene; see below) was immobilized on anti-PLK1 (4513; Cell Signaling)-coated high-binding 96-well plates and incubated with whole-cell extracts (see above) from immature DCs from donors with either the minor or major genotype for rs7262903 and rs7269320. MAVS that was associated with PLK1 was detected with anti-MAVS (3993; Cell Signaling), followed by incubation with HRP-conjugated anti-rabbit-IgG (7074; Cell Signaling) and addition of TMB substrate (Cell Signaling). After termination of the coloring reaction, the absorbance was measured at 450 nm.

Activation of TBK1, IKKε, IRF3, PLK1 and MST1. Phosphorylation of TBK1, IKKε, PLK1 and MST1 in HIV-1-infected DCs was detected 1 h (MST1) or 3 h (TBK1, IKKε, PLK1) post infection by flow cytometry. Cells were first fixed in 3% paraformaldehyde for 10 min and then permeabilized in 90% methanol at 4 °C for 30 min. Incubation of the primary antibodies anti-TBK1 p-Ser172 (1:50; 5483; Cell Signaling), anti-IKKε p-Ser172 (06-1340; Millipore), anti-PLK1 p-Thr210 (1:50; 5472; Cell Signaling) or MST1 p-Thr183 (1:50; 3681; Cell Signaling) was followed by incubation with phycoerythrin (PE)-conjugated anti-rabbit-Ig (1:200; 711-116-152; Jackson ImmunoResearch). Phosphorylation was analyzed on a FACS Calibur (BD).

Phosphorylated PLK1 was also detected by immunoblotting. 40 μg of whole-cell extracts (see above) were resolved by SDS–PAGE, and PLK1 was detected by immunoblotting with anti-PLK1 (1:1,000; 4513; Cell Signaling) or anti-PLK1 p-Thr210 (1:1,000; 5472; Cell Signaling), followed by incubation with HRP-conjugated secondary antibody (1:2,500; 21230; Pierce) and ECL detection (Pierce). To ensure that equal amounts of protein were used for immunoprecipitation, membranes were also incubated with anti-β-actin (1:2,000; sc-81178; Santa Cruz), followed by HRP-conjugated anti-mouse-IgG (1:1,000; sc-2314; Santa Cruz).

Flag–PLK1 (Origene) was captured on anti-FLAG (F1804; Sigma)-coated high-binding 96-wells plates and treated with 100 ng/ml recombinant active kinase (Raf-1, Millipore; MST1, Promega; PKA, Active Motif) in kinase activity buffer (50 mM Tris-HCl (pH 7.5), 10 mM $MgCl_2$, 50 μM DTT, 50 μM ATP, 25 mM β-glycerophosphate, 0.006% Brij-35) for 30 min at 30 °C. Thr210 phosphorylation was then detected with anti-PLK1 p-Thr210 (1:50; 5472; Cell Signaling), followed by incubation with HRP-conjugated anti-rabbit-IgG (1:1,000; 7074; Cell Signaling) and assayed using TMB substrate. Equal capture of Flag–PLK1 was determined with anti-PLK1 (1:100; 4513; Cell Signaling).

Nuclear translocation of IRF3 was determined in cytoplasmic (CE) and nuclear extracts (NE) of HIV-1-infected DCs prepared 3 h post infection using NucBuster protein extraction kit (Novagen). 10 μg CE and 20 μg NE were resolved by SDS–PAGE, and IRF3 was detected by immunoblotting with anti-IRF3 (1:500; sc-9082; Santa Cruz) and anti-IRF3 p-Ser396 (1:1,000; 29047; Cell Signaling), followed by incubation with HRP-conjugated secondary antibody (1:2,500; 21230; Pierce) and ECL detection (Pierce). Membranes were also probed with anti-RNAPII (1:1,000; clone CTD4H8; Millipore) or anti-β-actin (1:2,000; sc-81178; Santa Cruz), followed by HRP-conjugated anti-mouse-IgG (1:1,000; sc-2314; Santa Cruz) to ensure equal protein loading among CE and NE samples, respectively.

MST1 kinase activity was measured using an MST1 kinase enzyme system in combination with the ADP-Glo kinase assay (both from Promega). Whole-cell extracts containing the kinase were prepared at the indicated times using MST1 lysis buffer (25 mM Tris-HCl (pH 7.5), 25 mM $MgCl_2$, 2 mM EDTA, 250 μM DTT, 12.5 mM β-glycerophosphate, 1% Triton X-100, 10 μg/ml leupeptin, 10 μg/ml pepstatin A, 0.4 mM PMSF). MST1 was captured from 10 μg of extract using anti-MST1 (ab57836; Abcam)-coated high-binding 96-well plates. 5 μg substrate (Axltide) was added in 20 μl kinase activity buffer (see above) and incubated for 45 min at 30 °C. The ADP generated was then measured using the ADP-Glo kinase assay; the detected relative light units (RLU) are a measure for MST1 activity.

Translation initiation complex composition. Cytoplasmic extracts of HIV-1-infected DCs that were prepared 3 h post infection using ChIP lysis buffer (Active Motif) were treated with micrococcal nuclease (Cell Signaling) for 30 min at 37 °C. Translation initiation complexes were retained on m^7GTP–agarose (Jena Bioscience) from 40 μg of nuclease-treated extracts, using the cap analog m^7GpppG (New England BioLabs) as a competitor, as previously described[17], resolved by SDS–PAGE and detected by immunoblotting with anti-DDX3 (1:1,000; 2635; Cell Signaling), anti-MAVS (1:1,000; 3993; Cell Signaling), anti-eIF4G (1:1,000; 2498; Cell Signaling), anti-eIF4A (1:1,000; 2425; Cell Signaling) or anti-PABP (1:1,000; 4992; Cell Signaling), followed by incubation with HRP-conjugated secondary antibody (1:2,500; 21230; Pierce) and ECL detection (Pierce). To ensure that equal amounts of protein were used before m^7GTP cap binding, membranes were also incubated with anti-β-actin (1:2,000; sc-81178; Santa Cruz), followed by HRP-conjugated anti-mouse IgG (1:1,000; sc-2314; Santa Cruz).

RNA immunoprecipitation (RIP) assay. RIP and re-RIP assays were performed using EZ-MagnaRIP kit (Millipore). Briefly, DCs were fixed with 1% (vol/vol) paraformaldehyde and lysed. Protein–RNA complexes were immunoprecipitated from the equivalent of 1 million cells, using 2 μg anti-DDX3 (sc-98711; Santa Cruz), anti-MAVS (sc-68926; Santa Cruz), anti-eIF4G (2498; Cell Signaling) or a negative control IgG (sc-2027; Santa Cruz) and protein-G-coated magnetic beads. For re-RIP analyses, DDX3–RNA complexes were eluted from beads and desalted, and a second round of immunoprecipitation was performed with anti-MAVS or anti-eIF4G. RNA–protein cross-links were reversed in 200 mM NaCl for 2 h at 70 °C, before proteinase K treatment for 1 h at 37 °C. mRNA and non-mRNA fractions were separated, isolated and quantified as described, using strict controls to ensure that abortive HIV-1 RNA was measured in non-mRNA samples without cross-contamination with either genomic DNA or mRNA[12]. Primers are listed in **Supplementary Table 1**. To normalize for RNA input, a sample from each condition before immunoprecipitation was taken; results are expressed as percentage (%) input RNA.

Statistical analysis. Paired (mRNA, MST1) or unpaired (set point plasma viral load, MAVS–PLK1 ELISA) Student's *t*-test was used. Cox regression model was used for time-to-event outcomes, without controlling for multiple testing. Statistical significance was set at $P < 0.05$.

Data availability. The data that support the findings of this study are available from the corresponding author upon reasonable request.

44. Mesman, A.W. *et al.* Measles virus suppresses RIG-I-like receptor activation in dendritic cells via DC-SIGN-mediated inhibition of PP1 phosphatases. *Cell Host Microbe* **16**, 31–42 (2014).
45. Booiman, T., Setiawan, L.C. & Kootstra, N.A. Genetic variation in *Trex1* affects HIV-1 disease progression. *AIDS* **28**, 2517–2521 (2014).
46. Sarrami-Forooshani, R. *et al.* Human immature Langerhans cells restrict CXCR4-using HIV-1 transmission. *Retrovirology* **11**, 52 (2014).
47. Quakkelaar, E.D. *et al.* Susceptibility of recently transmitted subtype B human immunodeficiency virus type 1 variants to broadly neutralizing antibodies. *J. Virol.* **81**, 8533–8542 (2007).
48. Kinoshita, T. *et al.* Detection of mRNA for the *tax1* (*rex1*) gene of human T cell leukemia virus type I in fresh peripheral blood mononuclear cells of adult T cell leukemia patients and viral carriers by using the polymerase chain reaction. *Proc. Natl. Acad. Sci. USA* **86**, 5620–5624 (1989).